frontiers in Environmental Archaeology

TYPE Original Research
PUBLISHED 04 September 2026
DOI 10.3389/fearc.2026.1865397

OPEN ACCESS

EDITED BY
Alan Outram,
University of Exeter, United Kingdom

REVIEWED BY
Sónia Gabriel,
Laboratório de Arqueociências—Património Cultural, Portugal
Dongya Yang,
Simon Fraser University, Canada

*CORRESPONDENCE
Michael Buckley
m.buckley@manchester.ac.uk

RECEIVED 25 April 2026
REVISED 25 June 2026
ACCEPTED 06 July 2026
PUBLISHED 04 September 2026

CITATION
Buckley M, Elliott Smith EA, Oldfield E-M, Boulanger C, Kitchener AC, Concha FJ, Rick TC and Braje TJ (2026) Improving elasmobranch baselines in the California Channel Islands through ZooMS and stable isotope analyses.
Front. Environ. Archaeol. 5:1865397.
doi: 10.3389/fearc.2026.1865397

Improving elasmobranch baselines in the California Channel Islands through ZooMS and stable isotope analyses

Michael Buckley[1]*, Emma A. Elliott Smith[2,3], Ellie-May Oldfield[1], Clara Boulanger[4,5], Andrew C. Kitchener[6,7], Francisco J. Concha[8], Torben C. Rick[2] and Todd J. Braje[9]

[1]School of Natural Sciences, Manchester Institute of Biotechnology, University of Manchester, Manchester, United Kingdom, [2]Department of Anthropology, National Museum of Natural History, Smithsonian Institution, Washington, DC, United States, [3]Department of Biology and Center for Stable Isotopes, University of New Mexico, Albuquerque, NM, United States, [4]Institute of Archaeology, University College London, London, United Kingdom, [5]UMR 7194 Histoire Naturelle de L'Homme Préhistorique, Département Homme et Environnement, Muséum National D'Histoire Naturelle, Paris, France, [6]Department of Natural Sciences, National Museums Scotland, Edinburgh, United Kingdom, [7]School of Geosciences, University of Edinburgh, Edinburgh, United Kingdom, [8]Facultad de Ciencias del Mar y de Recursos Naturales, Universidad de Valparaíso, Viña del Mar, Chile, [9]Museum of Natural and Cultural History, University of Oregon, Eugene, OR, United States

Sharks are among the world's most endangered vertebrates, having declined by over 70% in abundance over the past 50 years—a collapse driven primarily by modern fishing. However, the extent of this impact is difficult to assess without improved records of past species distributions. Zooarchaeological records offer valuable baselines for shark diversity, distribution, and exploitation and provide essential historical context for assessing contemporary declines and vulnerability to extinction. Yet these records lag behind those for ray-finned fishes and marine mammals, largely because shark remains are difficult to identify to species level in the archaeological record. Here, we explore the use of Zooarchaeology by Mass Spectrometry (ZooMS) for species identification in this under-studied group, using an archaeological case study from the marine environments of Santa Rosa Island, California, USA. ZooMS analyses were paired with stable isotope analysis (SIA) for a subset of specimens, allowing us to assess both taxonomic resolution and past trophic ecology and habitat use of regional elasmobranchs. Of the 27 samples analysed that could not be identified beyond family level by morphological analysis, mostly as Triakidae (houndsharks) or Rajidae (skates), ZooMS grouped them into three distinct taxa that included the school shark (*Galeorhinus galeus*), leopard shark (*Triakis semifasciata*), and Pacific spiny dog shark (*Squalus suckleyi*). Among three additional samples morphologically identified as the Pacific angel shark (*Squatina californica*), two were confirmed but another distinct angel shark with a collagen fingerprint more closely resembling but distinct from the Chilean angel shark (*Squatina armata*) was also recovered—the latter possibly from a previously unknown species. Our findings demonstrate that ZooMS can distinguish between smoothhounds, leopard sharks, and other morphologically similar species and, when paired with stable isotope analysis, can reconstruct both the taxonomic composition and ecological structure of past shark communities. Furthermore, by demonstrating that ZooMS can detect species previously unknown to the

region, and potentially new to science, these results hold promise for reconstructing the historical composition of nearshore marine ecosystems and establishing appropriate historical baselines for the future management of at-risk species.

KEYWORDS

cartilage, Channel Islands archaeology, elasmobranch collagens, species identification, ZooMS

Introduction

Cartilaginous fishes, including elasmobranchs (sharks, skates, and rays), are an essential component of marine ecosystems, with many species (typically sharks) playing vital roles as keystone species and apex predators, which help maintain species diversity (Heithaus et al., 2022; Motivarash et al., 2020). Despite having existed for over 400 million years, they are among the world's most endangered vertebrate groups due to human impacts (overfishing, bycatch, habitat alteration, etc.) causing over 70% loss in abundance over the past 50 years (Pacoureau et al., 2021). Shark life histories are characterized by low fecundity, slow growth, late maturity, and relatively long-life spans, all of which makes them particularly vulnerable to population decline via anthropogenic threats such as overfishing, habitat degradation, and climate change (Dulvy et al., 2021; Sherman et al., 2023). In addition to increasingly being caught as bycatch, increases in shark exploitation are linked to declines in popular sport and recreational activity around bony fishes (Camhi, 2009) as well as rising demand within the international shark fin trade (Worm et al., 2024).

The historical ecology of elasmobranchs, especially sharks, demonstrates that humans have engaged with and harvested taxa across the world for millennia (Bom et al., 2020; Elliott Smith et al., 2023; Martínez-Candelas et al., 2020; Mojetta et al., 2018; Prieto, 2023). Utilizing historical perspectives of shark diversity and harvest patterns garnered through archaeology and other deep historical datasets make clear that worldwide species declines have been driven by human overfishing, with particular emphasis on loss over the past century (Bradshaw et al., 2008; Juan-Jordá et al., 2022; Roff et al., 2018). The absence of baseline data from pre-industrial eras often masks the true scale of these losses, leading to the 'shifting baseline syndrome' where modern depleted states are mistaken for historical norms. This relatively recent timescale for diversity loss presents challenges for building the long-term baselines needed in conservation decision-making, whereby historical patterns of species diversity, distribution (including habitat use), and community composition for many taxa are either understudied or unknown (Ferretti et al., 2018; Serena et al., 2020). This is particularly the case at century-to-millennia scales of comparison (e.g., Burg Mayer and De Freitas, 2023). Archaeology holds great promise for contributing to deep-time baselines and elucidating the antiquity of human engagements with elasmobranch taxa through the study of zooarchaeological specimens.

Robust zooarchaeological shark (and other elasmobranch taxa) assemblages have been recovered from many archaeological sites across the world but, in contrast to bony fish specimens and other types of marine vertebrate taxa, they are often difficult to identify beyond order, family, or genus based on morphology alone (Boulanger et al., 2025; Buckley et al., 2024; Royle et al., 2024). There are several reasons for this. Because chondrichthyan skeletons are composed of hyaline cartilage, with some elements only partly calcified, it is the vertebral centra, teeth, spines, and dermal denticles that are mostly preserved in archaeological deposits. Although these are the most readily identified shark parts, many of these elements are particularly difficult to identify to genus or species level based on morphology. For example, apart from a few shark species, it is often difficult to confidently make taxonomic identifications to genus or species based on shark vertebral or tooth morphology alone, particularly among specimens representing environments with high taxonomic diversity (e.g., tropical regions).

Species identification using ZooMS peptide mass fingerprinting

Biomolecular methods offer an objective solution to this issue of identification but have been largely underutilised for several reasons related to costs per sample, damage, and speed of interpretation. Although the analysis of ancient DNA is becoming increasingly more cost-effective (Seersholm et al., 2018), its greatest limitation is that of molecular preservation, whereby the few studies that have attempted to do so in shark remains typically yield low success rates (Shepherd and Campbell, 2021). Proteins on the other hand, particularly bone collagen, are thought to survive much longer, or at least better in warmer environments, such as those inhabited by many tropical shark species (Boulanger et al., 2025). Harnessing this greater longevity, a method of species identification by 'fingerprinting' collagen using mass spectrometry, referred to as 'ZooMS' (Zooarchaeology by Mass Spectrometry), was developed over a decade and a half ago (Buckley et al., 2010, 2009). Although initially focused on mammals, with occasional studies on reptiles (Guiry et al., 2024; Harvey et al., 2019), birds (Eda et al., 2020) and amphibians (Buckley and Cheylan, 2020), there has been a relatively large number of ZooMS applications to fish studies (Buckley et al., 2022, 2021; Guiry et al., 2020; Harvey et al., 2018; Richter et al., 2011; Winter et al., 2023) in comparison to the other 'lower vertebrate' groups.

However, there is a fundamental difference in the ZooMS fingerprint of elasmobranch remains in comparison to those of all other vertebrates, including other fish. This relates to the collagenous composition of the skeletal tissues being analysed. There are more than 28 types of collagen known to exist within humans at some point in life (Ricard-Blum, 2011), with 80–90%

of the collagen in mammals consisting of types I, II and III, of which type I collagen is by far the most abundant. Collagen types are most often represented by roman numerals to distinguish them from the numbered chains contained within each molecule of a given type. The triple helical structure common to all collagens is maintained through the presence of repeating amino acids proline (Pro) and its modified form, hydroxyproline (Hyp), which induces the twisting structure in each chain. Some collagen types are formed from three identical chains, with the cartilage-dominant type II collagen being a prime example. In contrast, the dominant type in bone, type I collagen, is made of genetically distinct chains, which in most vertebrates is made up of two identical (alpha 1) chains and one genetically distinct chain called the alpha 2. These alpha chains are often written as shorthand to the symbolised chain followed by its type in parentheses, so α1(I) and α2(I) for the dominant bone collagen. In bony ray-finned fishes, type I collagen is composed of three distinct chains, where the third [α3(I)] is a duplicate of the [α1(I)] gene (Morvan-Dubois et al., 2003). The latter of which does not exist in sharks and lampreys (Kimura and Ohno 1987) given the timing of the duplication event that gave rise to this (Harvey et al., 2021).

As their name suggests, the skeletal structure of cartilaginous fishes is primarily composed of cartilage. They do not develop osseous skeletons having secondarily lost the ability to produce endoskeletal bone (Coates et al., 1998). Elasmobranchs do develop a relatively thin outer layer of cortical mineralization over most of their skeleton (Seidel et al., 2016), a tissue typically characterised by type II collagen, a triple helical molecule made up of three identical alpha chains (COL2A1). The cartilaginous elements such as jaws, fins and vertebrae are covered by mineralised polygonal tiles called tesserae (Dean et al., 2009), which are more abundant in elasmobranchs but also increasingly recognised in holocephalans (Pears et al., 2020). It is the internal part of these tesserae, the round cells enclosed in lacunae, that contain the cartilaginous type II collagen (Chaumel et al., 2020), whereas the external parts located on the perichondral side are characterised by flatter cells that are engulfed in a type I collagen matrix (Ørvig, 1972) known as a fibrous perichondrium (Dean and Summers, 2006). Although dominated by type II collagen, type I collagen typical of bone is estimated to account for approximately one third of the total collagen content of shark cartilage (Rama and Chandrakasan, 1984), which should add a component to the use of ZooMS for species identification in archaeological remains that has only recently been explored (Boulanger et al., 2025; Buckley et al., 2024), so far only on a small fraction of known elasmobranch taxa.

Elasmobranchs of the California Channel Islands; environmental and archaeological context

The state of California encompasses a vast and ecologically diverse marine region, spanning over 840 miles (~1,352 km) of coastline. This expansive marine zone is characterized by complex oceanographic features, primarily driven by the interaction of major oceanic currents. The California Current transports cold, nutrient-rich water southward from the Gulf of Alaska, significantly influencing regional water temperatures. A critical biogeographic boundary occurs along Point Conception in southern California, just north of the Channel Islands within the Southern California Bight. At Point Conception, the southerly flowing currents of northern and central California meet northerly flowing countercurrents, creating a dynamic transition zone that supports a diverse array of marine life and distinct ecological habitats, including many elasmobranch taxa.

As of two decades ago, there were approximately 20 families, 30–31 genera, and 40–43 species of sharks and 10 families, 13 genera, and 22 species of batoids known in the waters of the California Coast (Ebert, 2003). Species diversity is highest in southern California, with Point Conception (Figure 1) serving as an approximate dividing line for more northerly and southerly species. In the warmer waters to the south of Point Conception, like the Channel Islands, the families and genera present are similar to those from the Mexican Coast (Ebert, 2003). The high productivity of this transition zone has supported human populations for millennia, potentially serving as a corridor for the initial peopling of the Americas. Some of the first peoples to enter the Americas may have traveled in boats following a 'kelp highway' and relied upon the highly productive kelp forest ecosystems stretching along the Pacific Rim (Erlandson et al., 2007). Along the California coast, archaeological records demonstrate that Indigenous communities harvested shellfish, sea mammals, and fish such as elasmobranchs for at least 10,000 years. These ancient maritime traditions established a foundation for the intensive use of marine resources that continued until and after first European contact (Braje et al., 2021).

The Late Holocene Native American village site on Santa Rosa Island, California, *Qshiwqshiw* (California trinomial: CA-SRI-85) is located on eastern Santa Rosa Island in an area with sandy beaches, rocky intertidal zones, and kelp forests that provided habitat and access to a variety of elasmobranchs and other fishes (Elliott Smith et al., 2023). Excavations at CA-SRI-85 were performed by Braje and colleagues, with details of the site, excavation procedures, and laboratory methods described in Braje et al. (2017) and Elliott Smith et al. (2023). Radiocarbon dates and artifacts recovered at the site document an occupation between 675 and 1,835 cal AD, with most of the site dating between 675 and 1,415 cal AD, just prior to initial contact with Europeans (Braje et al., 2017). The site contains house features, large and dense midden deposits and is part of a larger complex of sites associated with the Chumash village of *Qshiwqshiw*.

A robust sample of fish bones was identified by ichthyologist Dr. Ken Gobalet using comparative collections in his personal research collection and at the California Academy of Sciences, San Francisco, CA. Gobalet identified at least 23 species of fish at the site to the species level, including six elasmobranchs; 45 individual calcified cartilage elements to a specific species of shark (with 281 to the family level, in this case all to Triakidae), and 18 to two different species of batoid (with a further 340 to family level, in this case all Rajidae), with 52 to the coarse taxonomic level of Elasmobranchiomorphi (Elliott Smith et al., 2023). This is a robust assemblage of elasmobranchs from the Channel Islands, where assemblages are often dominated by bony fishes (>90% by NISP of assemblages).

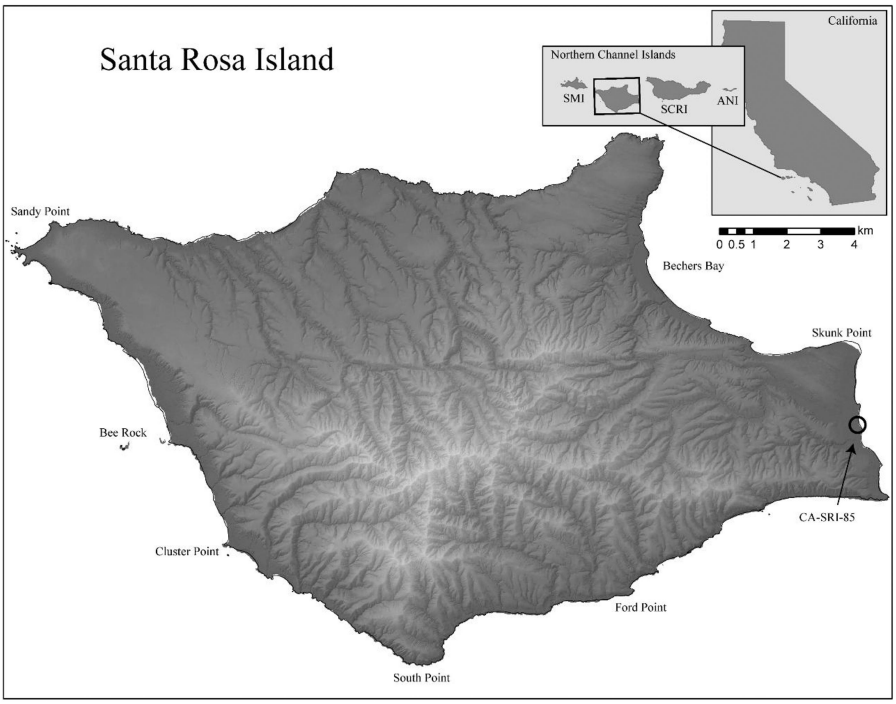

FIGURE 1
Map of Santa Rosa island (SRI) showing location of the CA-SRI-85 site, with the northern channel islands and their position along the California (USA); see Supplementary Figure S1 for other sites located on the SRI map with elasmobranch remains listed in Table 1.

The dense and well-preserved nature of the midden deposits and fish remains make it an ideal site for applying ZooMS, stable isotopes, and other analytical techniques to understand the historical ecology of elasmobranchs (Braje et al., 2017; Elliott Smith et al., 2023). Here, our aims were to explore the use of ZooMS for species identification among elasmobranch taxa, with an emphasis on sharks, using an archaeological case study of 31 specimens from CA-SRI-85 (Figure 1). To place the CA-SRI-85 ZooMS data and additional stable isotope analyses in context, we also synthesized all known archaeological occurrences of sharks, skates and rays in northern Channel Island archaeological sites and their relative abundance compared to bony fishes.

Materials and methods

Synthesizing archaeological elasmobranch remains from the northern Channel Islands

We performed a systematic literature search, including published and unpublished sources (reports in local archaeological repositories) to synthesize all archaeological elasmobranch occurrences for the northern Channel Islands, spanning the entire 13,000-year Indigenous occupation of the islands (Supplementary Table S1). The Number of Identified Specimens (NISP) and the relative abundance of NISP per all fishes identified to family, genus, and species, were tabulated. The taxonomy was standardized and updated following the World Register of Marine Species (WORMS). We could not check or confirm any identifications and have relied on those from the original analysts.

Faunal remains

The selection and analysis of modern specimens was based on establishing a modern baseline of species identification using ZooMS, whereas the zooarchaeological specimens were selected to confirm, refine, or refute previous identifications based on morphology. Modern skeletal tissues were obtained for 12 additional species to those previously published, including eight new genera (Supplementary Table S2). For ZooMS and isotope analyses, the specimens were selected from the modern skeletal comparative collection at the University of California Santa Barbara's (UCSB) zooarchaeological reference collection in the Department of Anthropology, with ZooMS identifications supported by further non-destructive polishing wipe samples taken from collections in the Division of Fishes at the Smithsonian's National Museum of Natural History and University of California Los Angeles (UCLA) reference collections. Specimens included vertebrae, teeth, as well as preserved cartilaginous materials and wipes samples. The zooarchaeological elasmobranch specimens (Supplementary Table S3) for the ZooMS study were selected from a subset of the remaining material from the isotopic analysis reported by Elliott Smith et al. (2023).

The specimens analysed here were drawn from the material remaining after isotopic study by Elliott Smith et al. (2023) and chosen to target taxa that dominate the CA-SRI-85 elasmobranch assemblage yet remain unresolved by morphology—primarily those that could be assigned only to the family level as Triakidae or Rajidae using traditional zooarchaeological morphology based identifications. Because these two family-level groupings account

10.3389/fearc.2026.1865397

TABLE 1 All sharks, skates, and rays identified in northern channel island (NCI) archaeological sites.

Taxon	All NCI sites (NISP)	CA-SRI-85 (NISP)	CA-SRI-85 per all NCI sites (%)
Elasmobranchii (sharks, skates, rays)	959	52	5.4
Heterodontidae			
Heterodontus francisci (horn shark)	1		
Alopiidae			
Alopias superciliosus (bigeye thresher)	1		
Lamnidae			
Isurus oxyrinchus (shortfin mako)	13	1	7.7
Lamna ditropis (salmon shark)	4		
Carcharhinidae (requiem sharks)	16		
Carcharhinus spp. (requiem sharks)	10		
Prionace glauca (blue shark)	2		
Scyliorhinidae	1		
Cephaloscyllium ventriosum (swell shark)	1		
Triakidae	701	281	40.1
Galeorhinus galeus (school shark)	111	11	9.9
Triakis semifasciata (leopard shark)	61		
Squalidae	149		
Squalus suckleyi (Pacific spiny dogfish)	142	2	1.4
Squatinidae			
Squatina californica (Pacific angel shark)	54	21	38.9
Batoidea	3		
Platyrhinidae			
Platyrhinoidis triseriata (thornback guitarfish)	36		
Torpedinidae	1		
Tetronarce californica (Pacific electric ray)	1		
Rhinobatidae	6		
Pseudobatos productus (shovelnose guitarfish)	9	3	33.3
Rajidae	348	340	97.7
Myliobatidae	2		
Myliobatis californica (California bat ray)	123	15	12.2
Urotrygonidae			
Urobatis halleri (round stingray)	10		
Total	2,765	726	26.3

Specific sites and time periods are available in Supplementary Table S1. Taxa were identified by morphology at CA-SRI-85 and the percentages they represent of all NCI remains identified to that category. Taxonomy follows World Register of Marine Species, and the order follows Weigmann et al. (2024).

for the majority of the assemblage ($n = 281$ and $n = 340$, respectively), they represent the categories that species-level identification by ZooMS would be most informative for.

The small number of specimens carrying prior species-level identifications reflects the design of the study to test ZooMS on material that could not be identified below the family level by morphology. These specimens constitute the bulk of the assemblage and where a biomolecular method offers the greatest gain. The few specimens that did carry a prior morphological identification—for example, the three assigned to the Pacific angel shark (*Squatina californica*)—provided an opportunistic check of ZooMS against morphology. Notably, one of these (SQCAL51) proved inconsistent with its morphological assignment, which underscores the value of this approach.

ZooMS collagen peptide mass fingerprinting

Approximately 25–50 mg of modern and archaeological tissues were processed for collagen peptide mass fingerprinting following Buckley (2013). In brief, 1 mL 0.6 M hydrochloric acid (HCl;

Sigma-Aldrich, UK) was added to each intact sample to enable decalcification and to induce repulsion between collagen fibrils [i.e., reasoning for why it has been used for non-mineralised tissues such as skins see Kirby et al. (2013)]. Note that for a small number ($n = 5$) of samples, collagen direct from stable isotope analyses (SIA in Supplementary Table S3) was used for ZooMS. Half of the acid-soluble fraction was then ultrafiltered into 50 mM ammonium bicarbonate (Sigma-Aldrich, UK), with two centrifugation steps (20 min; 12,400 rpm), and recovered in 0.1 mL solution. Additionally, ~1 mg of collagen samples from three additional archaeological taxa included as reference material (HEAL_1644, 1645 and 1695 from Royle et al. 2024) were resuspended in 50 mM ammonium bicarbonate and directly digested with trypsin following Guiry et al. (2020). Digests were then diluted 1/20 and 1 µL co-crystalised with 1 µL 10 mg/mL alpha-cyano hydroxycinnamic acid (Sigma-Aldrich, UK) in 50% acetonitrile (ACN)/0.1% trifluoroacetic acid (TFA) onto a stainless-steel Matrix Assisted Laser Desorption Ionization Time-of-Flight (MALDI-ToF) mass spectrometric target plate. Using a Bruker Rapiflex MALDI-ToF instrument at the Manchester Institute of Biotechnology (University of Manchester, UK), up to 20,000 laser shots were acquired over the mass/charge (m/z) range 700–3,700 and resultant spectra of archaeological samples categorised into distinct groupings based on mutual peak occurrence. Peaks that appeared diagnostic for each group, identified both manually and statistically using NEDMID (Baker et al., 2023), were then compared with those present in reference material within this study as well as from published studies (e.g., Buckley et al., 2024; Boulanger et al, 2025). and those with the highest number of peak matches indicating closest match. For selected peaks, MALDI-MS/MS was also attempted under conditions as above.

LC-MS/MS sequencing

Due to the high-level taxonomic uncertainty involved in some of the key taxa to this study [i.e., distinguishing batoid from shark in the case of 'Rajidae' (RJ) samples, among others], LC-MS/MS was carried out to add support to ZooMS identifications. Digested samples were analysed using an UltiMate® 3000 Rapid Separation LC (RSLC, Dionex Corporation, Sunnyvale, CA) coupled to a QE HF (Thermo Fisher Scientific, Waltham, MA) mass spectrometer at the UoM Biological Mass Spectrometry facility (University of Manchester, UK). Mobile phase A was 0.1% formic acid in water and mobile phase B was 0.1% formic acid in acetonitrile, and the column used was a 75 mm × 250 µm internal diameter 1.7 µM CSH C18, analytical column (Waters, UK). A 1 µL aliquot of the sample was transferred to a 5 µL loop and loaded on to the column at a flow of 300 nL/min for 5 min at 5% B. The loop was then taken out of line, and the flow was reduced from 300 nl/min to 200 nl/min in 0.5 min. Peptides were separated using a gradient from 5% to 18% B in 34.5 min, then from 18% to 27% B in 8 min and finally from 27% B to 60% B in 1 min. The column was washed at 60% B for 3 min before re-equilibration to 5% B in 1 min. At 55 min the flow was increased to 300nl/min until the end of the run at 60 min. Mass spectrometry data was acquired in a data directed manner for 60 min in positive mode. Peptides were selected for fragmentation automatically by data dependant analysis on a basis of the top 12 peptides with m/z between 300 and 1,750 Th and a charge state of 2, 3 or 4 with a dynamic exclusion set at 15 s. The MS Resolution was set at 120,000 with an AGC target of 3×10^6 and a maximum fill time set at 20 ms. The MS2 Resolution was set to 30,000, with an AGC target of 2×10^5, a maximum fill time of 45 ms, isolation window of 1.3 Th and a collision energy of 28. All data were collected in centroid mode. Raw files were then converted to mascot generic format (.MGF) files, which were searched against a locally curated database of elasmobranch collagen type 1 (COL1A1 and COL1A2) and type 2 (COL2A1) sequences obtained from the protein BLAST search of the elephant shark (*Callorhinchus milii*) as well as genome BLAST searches of selected elasmobranch taxa (see Supplementary Table S4) with 5 ppm peptide mass tolerance and 20 ppm fragment ion mass tolerance.

Stable isotope analysis

We report $\delta^{13}C$ and $\delta^{15}N$ values of bulk calcified cartilage protein for 16 elasmobranchs from UCSB comparative collections, and 29 specimens from CA-SRI-85 (Elliott Smith et al., 2023). Calcified tissue samples were demineralized with 0.25–0.5 M HCl at 5 °C for 48–120 h depending on sample size and density; acid was replaced as needed every 24 h. Samples were then rinsed in deionized H_2O, lyophilized, and lipid-extracted via three sequential 24 h soaks in 2:1 choloroform: methanol at room temperature. Lipid extracted samples were rinsed in deionized H_2O, lyophilized, and weighed to evaluate percent protein yield. Following this, 0.5–0.7 mg of each sample was sealed in a tin capsule for bulk tissue isotopic analysis.

Bulk cartilage protein $\delta^{13}C$ and $\delta^{15}N$ values, along with weight percent [C] and [N], were measured via Elemental Analyzer/Isotope Ratio Mass Spectrometry (EA-IRMS) using a Costech 4010 EA (Valencia, CA) coupled to a Thermo Scientific Delta V Plus IRMS (Bremen, Germany) at the University of New Mexico Center for Stable Isotopes (UNM-CSI; Albuquerque, NM). All samples and reference materials were calibrated against the internationally accepted standards for stable carbon and nitrogen isotope ratios, respectively Vienna-Pee Dee Belemnite (V-PDB) and atmospheric N_2. We report all isotopic data as δ values in parts per thousand, or per mil (‰), where $\delta^{13}C$ or $\delta^{15}N = 1{,}000*[(R_{samp}/R_{std})-1]$. Here, R_{samp} and R_{std} are the ^{13}C:^{12}C or ^{15}N:^{14}N ratios of the sample and standard, respectively. The standard deviations of organic in-house reference materials (milk casein and tuna muscle) were ≤ 0.2 ‰ for both $\delta^{13}C$ and $\delta^{15}N$ values. As a control for the quality of our collagen samples (Ambrose, 1990), we converted measured weight % [C]:[N] to atomic ratios via the following equation: $[C]:[N]_{atomic} = [C]:[N]_{weight} \times (14/12)$.

Results and discussion

Sharks, skates and rays in Channel Island archaeological sites

Our synthesis of sharks, skates and rays identified a NISP of 2,765 elasmobranch centra, dermal denticles, spines, and teeth

TABLE 2 LC-MS/MS search results against local database including collagen type I and II sequences of relevant genera, summarising number of ions and number of matches as well as protein scores and percentage sequence coverages for the top matches (peptides score information in Supplementary Tables S12–S18).

Sample	Group	# ions	COL1 match	Score/#unique matches (% coverage)	COL2 match	# Matches/score
TR25	1	32,272	*Galeorhinus*	31,173/961 (80%)	*Mustelus*[a]	14,393/493 (82%)
RJ35	2	22,479	*Squalus*	7,258/235 (56%)	*Squalus*	33,708/997 (85%)
MY22	3	28,016	*Myliobatis*	10,850/391 (38%)	*Hemitrygon*[a]	14,206/513 (75%)
TR1b7	4	35,609	*Mustelus*	31,190/971 (52%)	*Mustelus*	23,750/754 (82%)
TR23	4	29,996	*Mustelus*	14,732/532 (42%)	*Mustelus*	16,741/580 (80%)
SQ19B1	5	34,768	*Squatina*	15,907/596 (52%)	*Somniosus*[a]	30,990/436 (87%)
SQCAL5	6	24,248	*Squatina*	88,822/3,334 (57%)	*Squalus*[a]	8,409/436 (11%)

[a]Top COL2 match not the same as COL1 due to sequence gaps in source databases (showing amount of missing sequence for COL1/COL2 respectively: 35.4%/42.7% for *Squatina*; 4.9%/2.3% for *Mustelus*; 3.4%/48.2% for *Galeorhinus*; 26.4%/15.8% for *Myliobatis*; 7%/0.5% *Squalus*).

from all four of the northern Channel Islands (Table 2, Supplementary Table 3). Elasmobranchs were identified in 54 temporal components from 29 archaeological sites, including 10 sites on San Miguel Island, six on Santa Rosa Island, 11 on Santa Cruz Island, and two on Anacapa Island. The earliest securely dated elasmobranchs are from deposits at Daisy Cave dated to 10,150–8,480 cal BP, including triakids, angel shark, and unidentified elasmobranchs (Supplementary Table S1). Elasmobranchs also occur in early Holocene deposits on San Miguel Island at Cave of the Chimneys (CA-SMI-603) on Santa Cruz Island at CA-SCRI-109 and in six Middle Holocene sites (~7,500–4,000 years ago) on San Miguel and Santa Cruz Islands. The majority of all elasmobranchs occur in Late Holocene sites ($n = 21$) dated between ca. 4,000 and 200 years ago. Moreover, the 726 elasmobranch remains identified at CA-SRI-85 make up roughly 26.3% of all elasmobranchs identified on the northern Channel Islands (Table 2, Supplementary Table S1).

The elasmobranchs come from 13 different families, including sharks, skates, and rays. Some 15 species of elasmobranchs have been identified in northern Channel Island sites, dominated by sharks in the family Triakidae ($n = 701$), followed by skates and rays in the family Rajidae ($n = 348$), dogfish sharks in the family Squalidae and species spiny dogfish (*Squalus suckleyi*; $n = 290$), bat ray (*Myliobatis californica*; $n = 123$), school shark, also known as the Tope, Tope shark or soupfin shark (*Galeorhinus galeus*; $n = 111$), and all other species with less than 100 elements. Many researchers have noted similarities across elasmobranch species within and occasionally across different families, especially for vertebral centra [e.g., (Rick et al., 2002)]. Consequently, we urge caution when interpreting the species identifications presented here, especially since it is generally unclear if these were based on centra, teeth, dermal denticles or other elements, and suggest ZooMS as a future avenue to confirm or refute many of these identifications.

Taxonomic resolution of ZooMS in eastern Pacific elasmobranchs

The ability to retrieve species-level differences between the collagen peptide mass fingerprints for modern comparative specimens has been shown in several previous studies for requiem sharks (at least those of the genus *Carcharhinus*) and the hammerhead sharks (*Sphyrna*; Buckley et al., 2024; Boulanger et al, 2025). Likewise, we observe a similar level of taxonomic resolution for both the smoothhounds (*Mustelus*) and some of the angel sharks (*Squatina*), which are of greater relevance to elasmobranch taxa in the Eastern Pacific (Supplementary Figures S2–S6). However, caution should be placed to not imply that all taxa separated at the species level could be distinguished, which relates more to evolutionary divergence times and generation times, as discussed elsewhere (Buckley 2018). The apparent lack of amino acid differences between *Squalus acanthias* and *Squalus suckleyi* demonstrates this well, though the (COL1) sequences are only ~96% and 97% complete respectively (with COL2 being typically more conserved), and they are so closely related that it was only earlier this century they became considered distinct species (Ebert et al., 2010). Further caution should also be placed on the reliance on select few biomarkers alone (see Figure 2) without establishing homology through MS/MS interpretation (e.g., Supplementary Figure S7), hence our use of NEDMID in identifying markers from the grouped archaeological spectra.

Taxonomic identifications of archaeological remains using ZooMS

All the archaeological samples appeared to yield collagen fingerprints of suitable quality, spanning at least five distinct types of identifiable spectra (Figure 2). While most of these results derived from specimens that could not be morphologically identified below the family level, the ZooMS results reached species level in all cases where appropriate reference material was available [Supplementary Tables S5–S10 for NEDMID matches (in bold) of peak values between modern taxa and archaeological groupings; Supplementary Table S11 for markers by archaeological sample].

The 14 specimens identified as Triakidae were all apparently correct in their assignments, though the ZooMS results could more specifically match the majority ($n = 12$) to the school shark (*Galeorhinus galeus*), and the remaining ($n = 2$) as leopard shark (*Triakis semifasciata*). Interestingly, all nine of the morphologically identified 'Rajidae' were closest matched to the two 'Squalomorphi' sharks in our study that yielded somewhat similar fingerprints, the Pacific angel shark (*Squatina californica*)

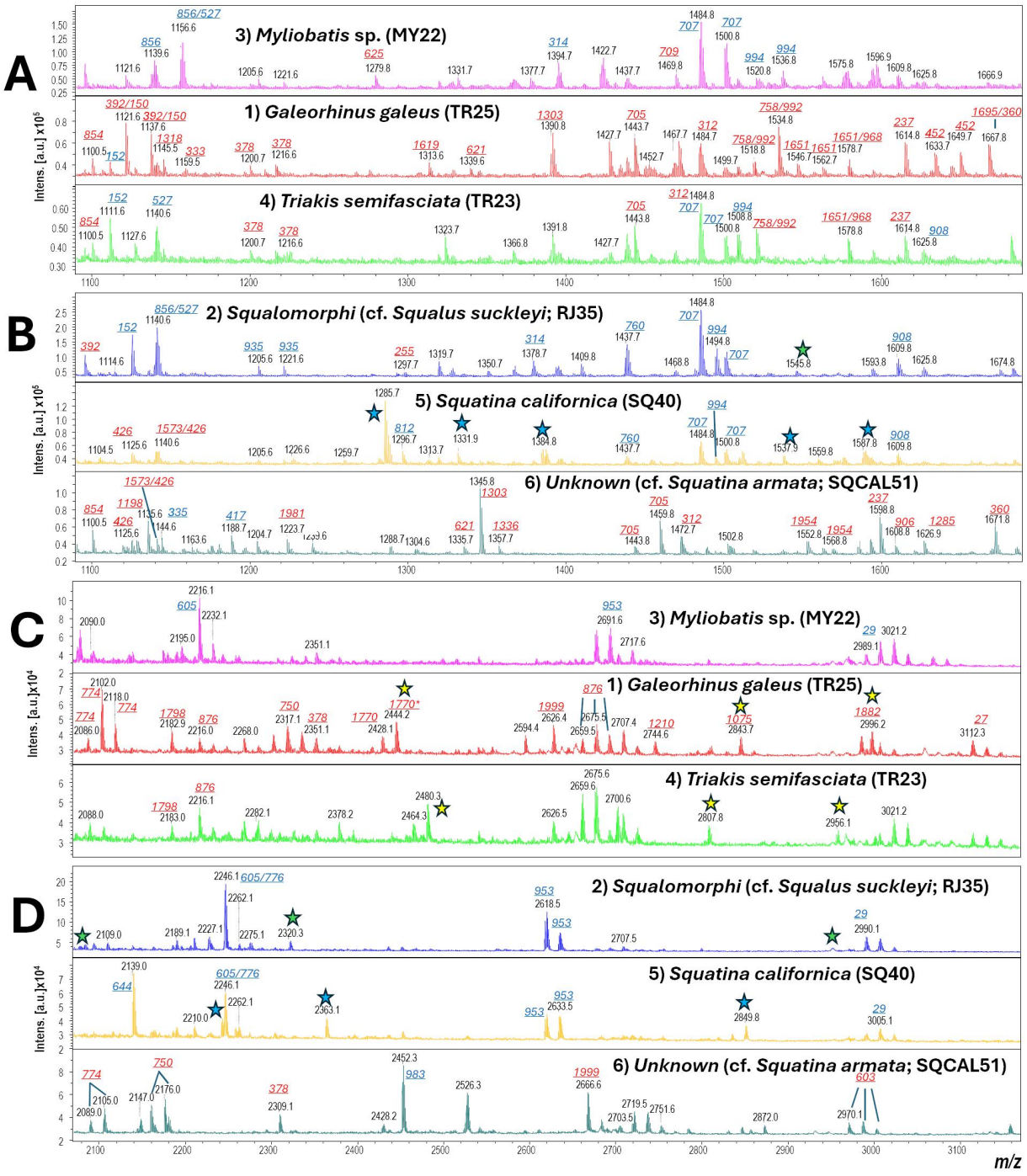

FIGURE 2
Zoomed in components of MALDI-ToF mass spectra of collagen digests from one representative sample of the six main taxonomic groups (Supplementary Table S11) identified in the archaeological remains split into lower **(A,B)** and higher **(C,D)** m/z ranges; presumed squalomorph spectra **(B,D)** are separated from myliobatis and the triakids **(A,C)**, with red numbers (starting amino acid of protein, two concatenated chains in the case of COL1) indicating matches to COL1 peptides and blue numbers to COL2 peptides [stars indicate selected biomarkers that were also observed in the respective reference spectra for triakids (yellow), squalus (green) and squatina (blue)].

and the Pacific spiny dogshark (*Squalus suckleyi*), with more peaks matching the latter. As expected, two of the three '*Squatina*' (SQ) samples (SQ19B1 and SQ40) were closest matching to *Squatina californica*, though the latter (SQ40) yielded several additional peaks of substantial relative intensity more closely matching the modern reference material); this potentially relates to the processing of the SQ19B1 sample for isotope analysis. However, the third (SQCAL51) yielded a fingerprint unlike any others in this study, including those of the original reference material for this study region, not explained by different processing approach due to the clear differences between SQCAL51 and SQ19B1. We therefore specifically processed SQCAL51 by LC-MS/MS sequencing for further exploration, along with one exemplar of the archaeological cf. *Squalus suckleyi* sample (RJ35)

due to the latter's morphological interpretation as Rajidae. With proteomic and morphological support for cf. *Squatina californica* (SQCAL51), we evaluated the fingerprints for the only known plausible member with a geographical range much further south in the eastern Pacific, the Chilean angel shark (*S. armata*). This latter comparison yielded a closer match, though not identical and therefore should not be considered a taxonomic match (Supplementary Figure S2). Lastly, the majority of the four 'Elasmobranch' identifications matched with the school shark, with one being matched also to the Pacific spiny dogshark. To lend further support to our taxonomic identifications by collagen fingerprinting, at least one each of the identified groupings was also processed by LC-MS/MS sequencing (Supplementary Tables S12–S18). In each case the top Mascot search results against the local database matched the closest expected taxon (Table 2), further supporting our identification of the 'Rajidae' specimens as deriving from angel sharks, despite the presence of at least six rajidae taxa within the sequence database. Note that for the triakidae sequence matches, *Triakis* has been shown to be phylogenetically closest to *Mustelus*, both forming a sister group to *Galeorhinus* (Winn et al., 2024).

However, the misidentifications of the Pacific spiny dogshark are not only at the family or even order level (Rajidae of the Rajiformes rather than Squalidae of the Squalomorphi sub-order of sharks), but at the much more basal divisions of sharks (Selachii) from batoids (Batomorphi, made up of rays, skates and sawfishes). Such misidentifications are likely not merely due to extrinsic factors such as analytical expertise and access to appropriate reference collections (Hawkins et al., 2022), but could be linked either to their relatively small size and/or the recent reclassification of Pacific spiny dog sharks as a separate species from *Squalus suckleyi* with some morphological differences in their more flattened skull shape, etc. We also acknowledge that ZooMS analyses are still in their infancy when it comes to the calcified cartilage tissues of elasmobranch remains, which pose significantly increased challenges compared with those of bone. The most notable of these is that due to the compositional differences between skeletal tissues (elements), which are expected to further differ between those of modern and ancient specimens of the same element (Supplementary Figure S5) rendering informatic approaches such as NEDMID less efficient as they are for bone. However, even though our results were limited by the sequence database with large amounts of missing sequence for *Squatina* (and this not the same species; *Squatina squatina*), with further genome-derived collagen sequences being increasingly available, supported by MS/MS data, defining more robust ZooMS markers for particular taxonomic groups will undoubtedly become simpler and more routine with time.

Isotope analyses of archaeological remains from CA-SRI-85

The comparative and archaeological specimens yielded well-preserved organic material for isotopic analysis (Figure 3). All UCSB reference individuals produced atomic C:N ratios within the accepted range for unaltered fish bone collagen [2.9–3.6; (Guiry and Szpak, 2021)], while five CA-SRI-85 specimens fell slightly above this range (3.7–3.8). However, these five specimens exhibited normal %N and produced isotopic values comparable to specimens with lower C:N ratios. These quality indicators confirm that both modern and archaeological collagen retain original biochemical signals, and hence these isotopic data provide a robust foundation for examining habitat use and ecological structure among sharks, skates, and rays.

The UCSB comparative collection, representing fishes from Santa Barbara, Ventura, and San Luis Obispo counties, provides an isotopic framework for characterizing the historical ecology of southern California elasmobranch communities. In this system, δ^{13}C values track the use of rocky-reef and kelp-forest habitats vs. soft or muddy substrates (e.g., Elliott Smith et al., 2023), while δ^{15}N values broadly reflect trophic position, ranging from low-trophic invertivores to piscivores. Reef-associated predators, including leopard sharks (*Triakis semifasciata*) and horn sharks (*Heterodontus francisci*), show the highest δ^{13}C values (−12.5 ‰ to −10.8 ‰), a pattern consistent with individuals feeding within kelp-influenced coastal habitats (Elliott Smith and Fox, 2021). The elevated δ^{13}C value of the single *H. francisci* specimen (UCSB 1.1) is consistent with its association with rocky reefs and kelp forest habitats, whereas its high δ^{15}N value is unexpected given the specimen's size (88 cm total length, typical of adults) and previous observations, which indicate frequent consumption of sea urchins by adults (Strong, 1989). However, the foraging ecology of *H. francisci* remains poorly known (Meese and Lowe, 2020), and strong home-range fidelity combined with a durophagous feeding strategy that can include higher-trophic-level invertebrates (e.g., crabs) could plausibly explain the elevated δ^{15}N value. Conversely, the soft-sediment coastal sharks, *Galeorhinus galeus*, *Mustelus* spp., *Cephaloscyllium ventriosum*, *Squalus suckleyi*, and *Squatina californica,* show lower δ^{13}C values (−13.5 ‰ to −12.7‰), reflecting their use of sandy and muddy benthic habitats with limited kelp input (Love, 2011). δ^{15}N values within this group vary from 14.2 ‰ to 16.1 ‰, likely reflecting subtle dietary differences among invertebrate feeders and more piscivorous taxa (Love, 2011). Skates and rays, including *Caliraja inornata*, *Urobatis halleri*, and *Myliobatis californica,* occupy a third zone defined by relatively low δ^{15}N (13.3 ‰ to 14.7 ‰) and δ^{13}C values (−13.8 ‰ to −12.6 ‰), consistent with invertebrate-dominated diets in sandy or muddy benthic environments (Love, 2011).

Linking ZooMS with isotope analyses of archaeological remains from SRI-85

Through the combined use of ZooMS and stable isotope analysis from modern and archaeological elasmobranchs, we can interpret the historical ecology of sharks, skates, and rays at CA-SRI-85, revealing broad agreement between the ecological patterns observed in the archaeological specimens and those documented in the UCSB comparative dataset. Because several UCSB comparative specimens lacked precise collection dates, bulk tissue δ^{13}C values were not Suess-corrected (e.g., Clark et al., 2021); accordingly, our interpretations emphasize relative patterns of enrichment and depletion rather than direct comparison of absolute values between archaeological and modern specimens. The specimens from CA-SRI-85 identified

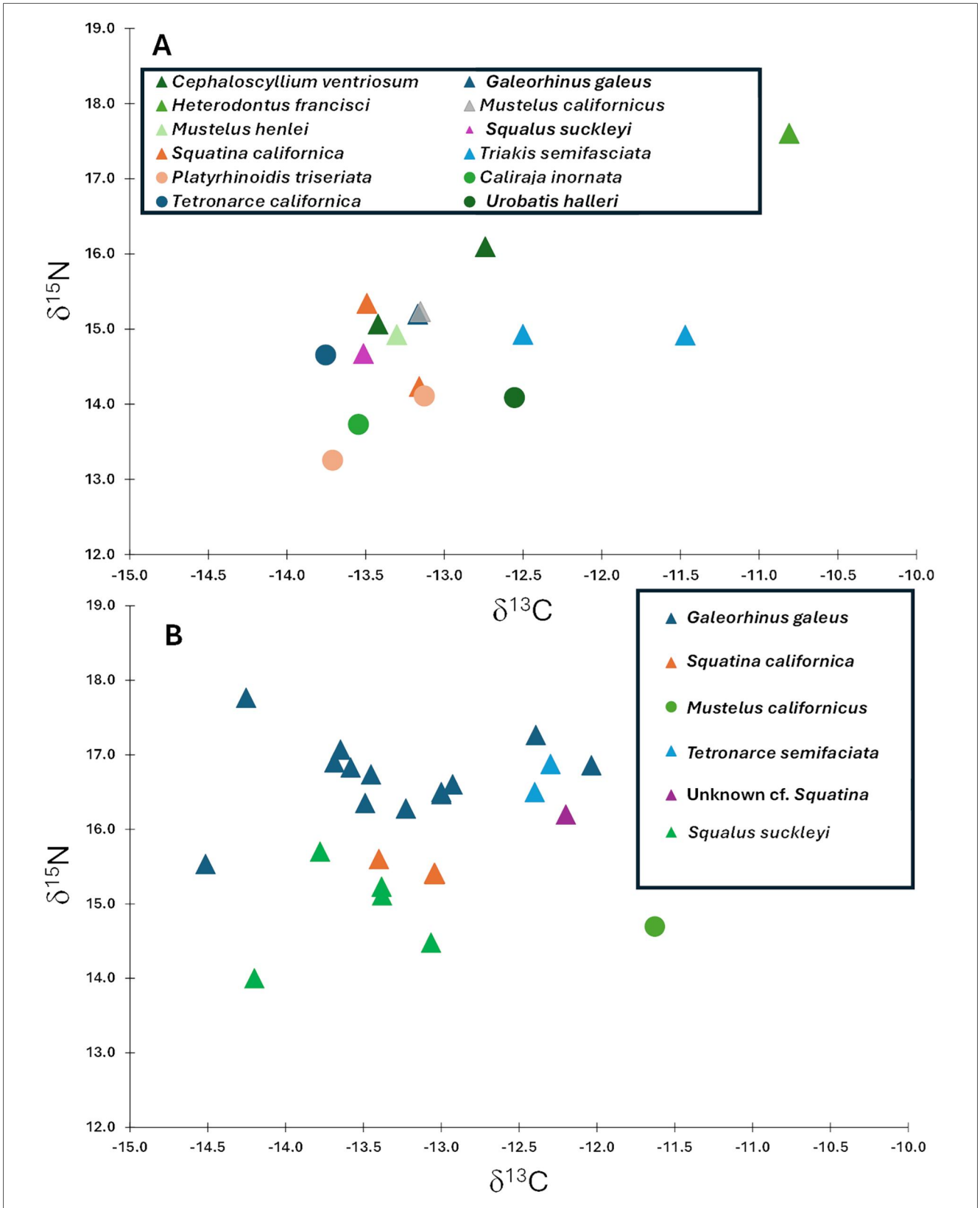

FIGURE 3
Bulk isotope ratios of carbon and nitrogen measured for **(A)** modern samples of different reference taxa and **(B)** ZooMS-identified archaeological samples from CA-SRI-85. Triangles denote sharks and circles denote skates or rays, with colour indicating species. Note that isotopic data in panel A have not been corrected for the Suess Effect (e.g., Clark et al., 2021; Cullen et al. 2001), given the lack of metadate for several specimens.

by ZooMS as leopard (Group 4) and school sharks (Group 1), for example, share nearly identical mean bulk tissue δ^{15}N values of roughly 16.5 ‰, indicating comparable trophic positions. However, these groups differ in mean bulk tissue δ^{13}C values by ~1 ‰, with leopard sharks more ^{13}C-enriched. This is in line with expected isotopic patterns for leopard shark individuals exploiting kelp-fringe habitats (Love, 2011; Smith, 2005) relative to the more soft-sediment, or pelagic species foraging typical of *Galeorhinus* (Lucifora et al., 2006), and mirrors the isotopic variance seen among these species in the modern UCSB comparative collections. This also helps explain patterns previously observed in compound-specific isotopic analyses from a subset of these same specimens (Elliott Smith et al., 2023), which documented substantial variability in basal carbon sources (e.g., habitat use) among archaeological elasmobranchs in the absence of species-level identifications. By applying ZooMS here, we can now attribute isotopic intraspecific ecological variability. Specimens identified as leopard sharks (TR23 and TR7) exhibited essential amino acid δ^{13}C values reflecting kelp forest foraging, whereas a specimen identified here as a school shark (TR25) had isotopic values closely aligned with phytoplankton fueled food webs.

Specimens identified as Pacific spiny dogsharks (c.f. *Squalus suckleyi;* Group 2) from CA-SRI-85 show lower δ^{15}N values (15 ‰) than leopard (*Triakis semifasciata*) and school (*Galeorhinus galeus*) sharks, with δ^{13}C values that overlap with the latter, pointing to sustained use of invertebrate prey from non-reef, soft-bottom habitats. Isotopic data for a single specimen identified as *Myliobatis californica* (Group 3) suggest low trophic level foraging on marine invertebrates (δ^{15}N = 14.7 ‰). The high δ^{13}C value (−11.6 ‰) of this specimen could reflect use of rocky kelp-forests habitats, or alternatively eelgrass beds, where bay rays are often found today (Lee et al., 2021). Further studies employing isotopic analysis of individual amino acids (e.g., Elliott Smith et al., 2022) would provide additional detailed information on past trophic levels of and carbon sources to archaeological elasmobranchs.

Taken together, the CA-SRI-85 isotopic data closely parallel the patterns seen in the modern comparative dataset. This alignment suggests that the ecological spacing among these species in southern California, specifically their relative trophic positions and habitat use, has not shifted significantly in recent times though we acknowledge that because the modern comparative material was not Suess-corrected, we should remain cautious with making direct comparisons between archaeological and modern specimens. The integration of ZooMS and isotopic analyses is critical to these insights: ZooMS resolves taxonomic identity with a precision not possible through morphology alone, while isotopic data provides direct evidence of trophic function and habitat use. In this case the latter also adds confidence to some of the subtle differences in peptide mass fingerprints observed for the same taxon, whether by incomplete enzymatic digestion (Boulanger et al., 2025; related to differences in protein abundance), or, a more evident issue with elasmobranchs than any other vertebrate, the presence of other collagen types in relatively high amounts (Buckley et al., 2024). In our study, some spectra, such as SQ40 and modern reference materials, yielded a dominance of a few additional peaks (e.g., *m/z* 2,139) shown to derive from type II collagen—apparently less abundant in some of the other archaeological samples such as SQ19B1, potentially reflecting the preferential loss of this protein during preparation for isotope methods. Yet the fact that the isotopic values for modern *Squalus* match up with those for the 'rajidae' specimens identified via ZooMS as *Squalus* further support their identifications (note that with only a few missing amino acids in both COL1 and COL2 sequences for both *Squalus acanthias* and *Squalus suckleyi*, no sequences differences were observed—unsurprising given that they were not long ago considered the same species). Somewhat in contrast, yet equally valuable in combination, is that the one of the few morphological identifications as *Squatina californica* (SQCAL51) was in disagreement with both ZooMS and isotope results, where the unexpected closest match to a distinct species satisfies all three approaches. However, although the closest match in this case to the Chilean angel shark (*Squatina armata*), not known this far north, there remain several notable (dominant) peak differences (*m/z*) between the reference *Squatina armata* and SQCAL51. Therefore, it is more plausible that this specimen reflects an as yet undescribed species of angel shark in the Pacific.

The fact that there appears greater variation between the modern reference spectra of *Squatina* species of the eastern Pacific (*Squatina californica* and *Squatina armata*) than between the former and *Squalus* warrants further investigation with future genomic support, but collagen fingerprints have long been known to not reflect hierarchically accurate topologies across all taxonomic groups (e.g., see *Rangifer* within Artiodactyls; Buckley et al., 2009). Ideally our analyses would have involved attempts of aDNA analysis but given the nature of ZooMS sample selection being influenced by what had been already extensively destructively sampled for isotope analyses, such a validation attempt was not feasible in this case. Furthermore, the antiquity of the SRI assemblages being substantially older than other known successful aDNA attempts on cartilaginous fish remains (e.g., Shepherd and Campbell, 2021), even dedicated analyses independent of sampling for isotopes would likely result in relatively low success rates. Yet both lines of validation, whether through aDNA of elasmobranch taxa from other assemblages (see Supplementary Figures S4, S6 for inclusion of available archaeological triakid reference material from Royle et al., 2024), and/or more relevant taxa having their genome sequenced for searching against using the LC-MS/MS datasets provided here, will undoubtedly improve with time. These DNA-based improvements could also enable future investigations into how the relative proportions of the two collagen types preserve deeper into the archaeological record with increasing antiquity. For example, in contrast to a near even ratio of type I and type II collagen peptides in modern samples, the archaeological spectra (e.g., Figure 2) appear to show some biases—more type I in the triakids but more type II in the squalomorphs, changes that could warrant consideration of in terms of biomarker usage. Similarly, analysts would also need to take into account how different collagen extraction methods, such as the use of different acids and protein solubilization and subsequent purification steps could be affected by such diagenetic changes in cartilaginous samples (this is the main reason we included LC-MS/MS analyses of different methods applied to 'group 4').

Nonetheless, this distinct fingerprint in the archaeological groupings also explains the morphological identification and

these discrepancies with the analytical approaches. Overall, the convergence of these two lines of evidence yields a high-resolution reconstruction of shark, skate, and ray ecology at CA-SRI-85 and reveals long-term continuity in the ecological niches these taxa occupy within nearshore food webs.

Conclusions

This work represents the first synthesis for understanding shark, skate, and ray fisheries on the northern Channel Islands across the Holocene. Zooarchaeological data document a robust assemblage of some 2,765 elasmobranch remains from the islands, but nearly 80% of these are identified only to genus, family or higher taxonomic categories, including 959 (35% of all elasmobranchs) identified simply as elasmobranch. Although only a subset of the full archaeological assemblage from CA-SRI-85 was tested, the majority of the samples analysed here for ZooMS were those that could not be identified beyond family level by morphological analysis, mostly as Triakidae or Rajidae. Yet these family-level groupings represent the majority of the elasmobranch assemblage ($n = 281$ and $n = 340$ respectively), i.e., 38% and 46% for these two families. Along with the 7% 'Elasmobranch' level identifications, this equates to >91% of the elasmobranch assemblage. In addition to this, given that the 'Rajidae' reflect nearly half of the elasmobranch assemblage, and these were all shown not to be from this family, this demonstrates the significance of ZooMS collagen peptide mass fingerprinting on such interpretations.

Overall, along with retrieving a collagen fingerprint for the already known *Myliobatis* specimen, we identified five distinct taxa within a zooarchaeological assemblage from Santa Rosa Island (CA-SRI-85), including the school shark (*Galeorhinus galeus*), leopard shark (*Triakis semifasciata*), the Pacific spiny dogshark (*Squalus suckleyi*), the Pacific angel shark (*Squatina californica*) and one individual of another angel shark with closest signatures to the Chilean angel shark (*Squatina armata*). If substantiated, the latter would either reflect the northernmost of its kind known for this species, though given the inexact match it more likely reflects biomolecular indication of the presence of an as yet unknown species, in either case demonstrating the clear potential for ZooMS in better understanding species palaeobiogeography, including local extirpations, which is more significant for this poorly understood taxonomic group. Furthermore, our findings demonstrate potential for ZooMS to distinguish not only between smoothhounds and the leopard sharks, but also between smoothhound species. These results are particularly promising for better understanding the deep historical composition of nearshore marine ecosystems and for building appropriate historical baselines for the future management of these at-risk species. However, we reiterate the acknowledgement of several important limitations discussed throughout this study, including: (1) incomplete reference coverage in terms of collagen peptide mass fingerprints, (2) missing sequences of key taxa in attempts to use LC-MS/MS analyses to corroborate peptide biomarkers and/or taxonomic assignment, (3) tissue-specific collagen variability related to preservation, and (4) the still-developing state of ZooMS applications to calcified cartilage samples with respect to method optimisation that includes validation.

Data availability statement

The datasets presented in this study can be found in online repositories. The names of the repository/repositories and accession number(s) can be found in the article/Supplementary Material.

Ethics statement

Ethical approval was not required for the study involving animals in accordance with the local legislation and institutional requirements because only skeletal material already present in reference collections were used.

Author contributions

MB: Conceptualization, Data curation, Formal analysis, Investigation, Methodology, Project administration, Resources, Supervision, Validation, Visualization, Writing – original draft, Writing – review & editing. ES: Data curation, Formal analysis, Investigation, Methodology, Resources, Visualization, Writing – original draft. E-MO: Formal analysis, Investigation, Methodology, Writing – review & editing. CB: Investigation, Validation, Visualization, Writing – review & editing. AK: Resources, Writing – review & editing. FC: Resources, Writing – review & editing. TR: Conceptualization, Data curation, Investigation, Project administration, Resources, Validation, Writing – review & editing. TB: Data curation, Project administration, Resources, Validation, Writing – review & editing.

Funding

The author(s) declared that financial support was not received for this work and/or its publication.

Acknowledgments

MB thanks assistance of undergraduate student Hannah Coveney in lab pretreatments of modern reference material. EES thanks Chris Cutter for his help in preparing UCSB comparative samples for isotopic analysis, and Seth Newsome, Laura Burkemper and Viorel Atudorei for providing laboratory space and general support in conducting isotopic analyses. We also thank Sara McClure at the University of California Santa Barbara and Tom Wake at the University of California Los Angeles for providing reference material from the UCSB and UCLA Zooarchaeology comparative collections, respectively, as well as Eric Guiry of Simon Fraser University for providing collagen reference material from a previous publication. We thank the Division of Fishes, especially Jeff Clayton, at the National Museum of Natural History, Smithsonian Institution

for providing access to swipe specimens for reference material. Fieldwork at CA-SRI-85 was supported by the National Park Service, especially Ann Huston and Kelly Minas and conducted in concert with Chumash consultants.

Conflict of interest

The author(s) declared that this work was conducted in the absence of any commercial or financial relationships that could be construed as a potential conflict of interest.

The author MB declared that they were an editorial board member of Frontiers, at the time of submission. This had no impact on the peer review process and the final decision.

The handling editor AO declared a past co-authorship with the author AK.

Generative AI statement

The author(s) declared that generative AI was not used in the creation of this manuscript.

Any alternative text (alt text) provided alongside figures in this article has been generated by Frontiers with the support of artificial intelligence and reasonable efforts have been made to ensure accuracy, including review by the authors wherever possible. If you identify any issues, please contact us.

Publisher's note

Supplementary material

The Supplementary Material for this article can be found online at: https://www.frontiersin.org/articles/10.3389/fearc.2026.1865397/full#supplementary-material

References

Ambrose, S. H. (1990). Preparation and characterization of bone and tooth collagen for isotopic analysis. *J. Archaeol. Sci.* 17, 431–451. doi: 10.1016/0305-4403(90)90007-R

Baker, A., Harvey, V. L., and Buckley, M. (2023). Machine learning for collagen peptide biomarker determination in the taxonomic identification of archaeological fish remains. *J. Archaeol. Sci. Rep.* 49, 104001. doi: 10.1016/j.jasrep.2023.104001

Bom, R. A., Van De Water, M., Camphuysen, K. C. J., Van Der Veer, H. W., and Van Leeuwen, A. (2020). The historical ecology and demise of the iconic Angelshark Squatina squatina in the southern north sea. *Mar. Biol.* 167, 91. doi: 10.1007/s00227-020-03702-0

Boulanger, C., Ono, R., Intoh, M., and Buckley, M. (2025). ZooMS as a tool for understanding prehistoric pelagic fishing: insights from archaeological shark and scombrid remains on Fais Island, Micronesia, over the last two millennia. *J. Archaeol. Sci.* 184, 106386. doi: 10.1016/j.jas.2025.106386

Bradshaw, C. J. A., Fitzpatrick, B. M., Steinberg, C. C., Brook, B. W., and Meekan, M. G. (2008). Decline in whale shark size and abundance at Ningaloo reef over the past decade: the world's largest fish is getting smaller. *Biol. Conserv.* 141, 1894–1905. doi: 10.1016/j.biocon.2008.05.007

Braje, T. J., Erlandson, J. M., and Rick, T. C. (2021). *Islands Through Time: A Human and Ecological History of California's Northern Channel Islands*. California: Bloomsbury Publishing PLC.

Braje, T. J., Rick, T. C., Szpak, P., Newsome, S. D., McCain, J. M., Smith, E., et al. (2017). Historical ecology and the conservation of large, hermaphroditic fishes in Pacific coast kelp forest ecosystems. *Sci. Adv.* 3, e1601759. doi: 10.1126/sciadv.1601759

Buckley, M. (2013). A molecular phylogeny of plesiorycteropus reassigns the extinct mammalian order 'Bibymalagasia.'. *PLoS One* 8, e59614. doi: 10.1371/journal.pone.0059614

Buckley, M., and Cheylan, M. (2020). Collagen fingerprinting for the species identification of archaeological amphibian remains. *Boreas* 49, 709–717. doi: 10.1111/bor.12443

Buckley, M., Collins, M., Thomas-Oates, J., and Wilson, J. C. (2009). Species identification by analysis of bone collagen using matrix-assisted laser desorption/ionisation time-of-flight mass spectrometry. *Rapid Commun. Mass Spectrom.* 23, 3843–3854. doi: 10.1002/rcm.4316

Buckley, M., Harvey, V. L., Petiffer, D., Russ, H., Wouters, W., and Van Neer, W. (2022). Medieval fish remains on the newport ship identified by ZooMS collagen peptide mass fingerprinting. *Archaeol. Anthropol. Sci.* 14, 41. doi: 10.1007/s12520-021-01478-y

Buckley, M., Oldfield, E.-M., Oliveira, C., Boulanger, C., Kitchener, A. C., Fuller, N. R., et al. (2024). Species identification of modern and archaeological shark and ray skeletal tissues using collagen peptide mass fingerprinting. *Front. Mar. Sci* 11, 1500595. doi: 10.3389/fmars.2024.1500595

Buckley, M., Pinsonneault, M., Brassey, C., and Rolett, B. (2021). High-throughput MicroCT and ZooMS collagen fingerprinting of scombrid bone from the Marquesas islands. *J. Archaeol. Sci.* 136, 105475. doi: 10.1016/j.jas.2021.105475

Buckley, M., Whitcher Kansa, S., Howard, S., Campbell, S., Thomas-Oates, J., and Collins, M. (2010). Distinguishing between archaeological sheep and goat bones using a single collagen peptide. *J. Archaeol. Sci.* 37, 13–20. doi: 10.1016/j.jas.2009.08.020

Buckley, M. (2018). "Zooarchaeology by mass spectrometry (ZooMS) collagen fingerprinting for the species identification of archaeological bone fragments," in *Zooarchaeology in Practice: Case Studies in Methodology and Interpretation in Archaeofaunal Analysis*, eds. C. M. Giovas, and M. J. LeFebvre (Cham: Springer International Publishing), 227–247.

Burg Mayer, G., and De Freitas, R. H. A. (2023). Archaeological sharks: changes in the trophic ecology between late holocene and modern shark communities in south Brazil. *Mar. Biol.* 170, 102. doi: 10.1007/s00227-023-04252-x

Camhi, M. D. (2009). *The Conservation status of Pelagic Sharks and Rays: Report of the IUCN Shark Specialist Group : Pelagic Shark Red List Workshop, Tubney House, University of Oxford, UK, 19–23 February 2007*. Newbury, UK: IUCN Species Survival Commission's Shark Specialist Group.

Chaumel, J., Schotte, M., Bizzarro, J. J., Zaslansky, P., Fratzl, P., Baum, D., et al. (2020). Co-aligned chondrocytes: zonal morphological variation and structured arrangement of cell lacunae in tessellated cartilage. *Bone* 134, 115264. doi: 10.1016/j.bone.2020.115264

Clark, C. T., Cape, M. R., Shapley, M. D., Mueter, F. J., Finney, B. P., and Misarti, N. (2021). SuessR: regional corrections for the effects of anthropogenic CO2 on δ13C data from marine organisms. *Methods Ecol. Evol.* 12, 1508–1520. doi: 10.1111/2041-210X.13622

Coates, M. I., Sequeira, S. E. K., Sansom, I. J., and Smith, M. M. (1998). Spines and tissues of ancient sharks. *Nature* 396, 729–730. doi: 10.1038/25467

Cullen, J. T., Rosenthal, Y., and Falkowski, P. G. (2001). The effect of anthropogenic CO2 on the carbon isotope composition of marine phytoplankton. *Limnol. Oceanogr.* 46, 996–998. doi: 10.4319/lo.2001.46.4.0996

Dean, M. N., and Summers, A. P. (2006). Mineralized cartilage in the skeleton of chondrichthyan fishes. *Zoology* 109, 164–168. doi: 10.1016/j.zool.2006.03.002

Dean, M. N., Mull, C. G., Gorb, S. N., and Summers, A. P. (2009). Ontogeny of the tessellated skeleton: insight from the skeletal growth of the round stingray urobatis halleri. *J. Anat.* 215, 227–239. doi: 10.1111/j.1469-7580.2009.01116

Dulvy, N. K., Pacoureau, N., Rigby, C. L., Pollom, R. A., Jabado, R. W., Ebert, D. A., et al. (2021). Overfishing drives over one-third of all sharks and rays toward a global extinction crisis. *Curr. Biol.* 31, 4773–4787.e8. doi: 10.1016/j.cub.2021.08.062

Ebert, D. A. (2003). *Sharks, Rays, and Chimaeras of California (California Natural History Guides)*. Berkeley, CA: University of California Press.

Ebert, D. A., White, W. T., Goldman, K. J., Compagno, L. J. V., Daly-Engel, T. S., and Ward, R. D. (2010). Resurrection and redescription of *Squalus suckleyi* (girard, 1854) from the north Pacific, with comments on the *Squalus acanthias* subgroup (squaliformes: squalidae). *Zootaxa* 2612, 22–40. doi: 10.11646/zootaxa.2612.1.2

Eda, M., Morimoto, M., Mizuta, T., and Inoué, T. (2020). ZooMS for birds: discrimination of Japanese archaeological chickens and indigenous pheasants using collagen peptide fingerprinting. *J. Archaeol. Sci. Rep.* 34, 102635. doi: 10.1016/j.jasrep.2020.102635

Elliott Smith, E. A., Braje, T. J., Gobalet, K. W., Campbell, B., Newsome, S. D., and Rick, T. C. (2023). Archaeological and stable isotope data reveal patterns of fishing across the food web on California's Channel Islands. *Holocene* 33, 446–458. doi: 10.1177/09596836221145383

Elliott Smith, E. A., Fox, M. D., Fogel, M. L., and Newsome, S. D. (2022). Amino acid δ13C fingerprints of nearshore marine autotrophs are consistent across broad spatiotemporal scales: an intercontinental isotopic dataset and likely biochemical drivers. *Funct. Ecol.* 36, 1191–1203. doi: 10.1111/1365-2435.14017

Elliott Smith, E., and Fox, M. (2022). Characterizing energy flow in kelp forest food webs: a geochemical review and call for additional research. *Ecography* 2022, e05566. doi: 10.1111/ecog.05566

Erlandson, J. M., Graham, M. H., Bourque, B. J., Corbett, D., Estes, J. A., and Steneck, R. S. (2007). The kelp highway hypothesis: marine ecology, the coastal migration theory, and the peopling of the Americas. *J. Isl. Coast. Archaeol.* 2, 161–174. doi: 10.1080/15564890701628612

Ferretti, F., Curnick, D., Liu, K., Romanov, E. V., and Block, B. A. (2018). Shark baselines and the conservation role of remote coral reef ecosystems. *Sci. Adv.* 4, eaaq0333. doi: 10.1126/sciadv.aaq0333

Guiry, E. J., Buckley, M., Orchard, T. J., Hawkins, A. L., Needs-Howarth, S., Holm, E., et al. (2020). Deforestation caused abrupt shift in great lakes nitrogen cycle. *Limnol. Oceanogr.* 65, 1921–1935. doi: 10.1002/lno.11428

Guiry, E. J., and Szpak, P. (2021). Improved quality control criteria for stable carbon and nitrogen isotope measurements of ancient bone collagen. *J. Archaeol. Sci.* 132, 105416. doi: 10.1016/j.jas.2021.105416

Guiry, E., Kennedy, J. R., Malcom, C., Miller, M., Hall, O., Buckley, M., et al. (2024). Archaeological evidence for long-term human impacts on sea turtle foraging behaviour. *R. Soc. Open. Sci.* 11, 240120. doi: 10.1098/rsos.240120

Harvey, V. L., Daugnora, L., and Buckley, M. (2018). Species identification of ancient Lithuanian fish remains using collagen fingerprinting. *J. Archaeol. Sci.* 98, 102–111. doi: 10.1016/j.jas.2018.07.006

Harvey, V. L., Keating, J. N., and Buckley, M. (2021). Phylogenetic analyses of ray-finned fishes (Actinopterygii) using collagen type I protein sequences. *R. Soc. Open. Sci.* 8, 201955. doi: 10.1098/rsos.201955

Harvey, V. L., LeFebvre, M. J., Defrance, S. D., Toftgaard, C., Drosou, K., Kitchener, A. C., et al. (2019). Preserved collagen reveals species identity in archaeological marine turtle bones from Caribbean and Florida sites. *R. Soc. Open. Sci.* 6, 191137. doi: 10.1098/rsos.191137

Hawkins, A. L., Buckley, M., Needs-Howarth, S., and Orchard, T. J. (2022). Practice makes perfect? Inter-analyst variation in the identification of fish remains from archaeological sites. *Int. J. Osteoarchaeol.* 32, 694–705. doi: 10.1002/oa.3096

Heithaus, M. R., Dunn, R. E., Farabaugh, N. F., Lester, E., Madin, E., Meekan, M. G., et al. (2022). *Advances in Our Understanding of the Ecological Importance of Sharks and Their Relatives, in: Biology of Sharks and Their Relatives*. Boca Raton, FL: CRC Press.

Juan-Jordá, M. J., Murua, H., Arrizabalaga, H., Merino, G., Pacoureau, N., and Dulvy, N. K. (2022). Seventy years of tunas, billfishes, and sharks as sentinels of global ocean health. *Science* 378, eabj0211. doi: 10.1126/science.abj0211

Kimura, S., and Ohno, Y. (1987). Fish type I collagen: tissue-specific existence of two molecular forms, and α1α2α3, in Alaska pollack. *Comp. Biochem. Physiol. B Comp. Biochem.* 88 (2), 409–413. doi: 10.1016/0305-0491(87)90320-8

Kirby, D. P., Buckley, M., Promise, E., Trauger, S. A., and Holdcraft, T. R. (2013). Identification of collagen-based materials in cultural heritage. *Analyst* 138, 4849–4858. doi: 10.1039/C3AN00925D

Lee, C.-L., Lin, W.-J., Liu, P.-J., Shao, K.-T., Lin, H.-J., Lee, C.-L., et al. (2021). Highly productive tropical seagrass beds support diverse consumers and a large organic carbon pool in the sediments. *Diversity. (Basel)* 13, 544. doi: 10.3390/d13110544

Love, M. S. (2011). *Certainly More Than You Want to Know About the Fishes of the Pacific Coast: A Postmodern Experience*. Santa Barbara, CA: Really Big Press.

Lucifora, L. O., García, V. B., Menni, R. C., and Escalante, A. H. (2006). Food habits, selectivity, and foraging modes of the school shark *Galeorhinus galeus*. *Mar. Ecol. Prog. Ser.* 315, 259–270 doi: 10.3354/meps315259

Martínez-Candelas, I. A., Pérez-Jiménez, J. C., Espinoza-Tenorio, A., McClenachan, L., and Méndez-Loeza, I. (2020). Use of historical data to assess changes in the vulnerability of sharks. *Fish. Res.* 226, 105526. doi: 10.1016/j.fishres.2020.105526

Meese, E. N., and Lowe, C. G. (2020). Active acoustic telemetry tracking and tri-axial accelerometers reveal fine-scale movement strategies of a non-obligate ram ventilator. *Mov. Ecol.* 8, 8. doi: 10.1186/s40462-020-0191-3

Mojetta, A. R., Travaglini, A., Scacco, U., and Bottaro, M. (2018). Where sharks met humans: the Mediterranean sea, history and myth of an ancient interaction between two dominant predators. *Region. Stud. Marine Sci.* 21, 30–38. doi: 10.1016/j.rsma.2017.10.001

Morvan-Dubois, G., Le Guellec, D., Garrone, R., Zylberberg, L., and Bonnaud, L. (2003). Phylogenetic analysis of vertebrate fibrillar collagen locates the position of zebrafish α3 (I) and suggests an evolutionary link between collagen α chains and hox clusters. *J. Mol. Evol.* 57 (5), 501–514. doi: 10.1007/s00239-003-2502-x

Motivarash, Y., Fofandi, D., Rehanavaz, M., Kariya, P., and Dabhi, R. (2020). Importance of sharks in ocean ecosystem. *J. Entomol. Zool. Stud.* 8, 611–613.

Ørvig, T. (1972). The latero-sensory component of the dermal skeleton in lower vertebrates and its phyletic significance. *Zool. Scr.* 1, 139–155. doi: 10.1111/j.1463-6409.1972.tb00672.x

Pacoureau, N., Rigby, C. L., Kyne, P. M., Sherley, R. B., Winker, H., Carlson, J. K., et al. (2021). Half a century of global decline in oceanic sharks and rays. *Nature* 589, 567–571. doi: 10.1038/s41586-020-03173-9

Pears, J. B., Johanson, Z., Trinajstic, K., Dean, M. N., and Boisvert, C. A. (2020). Mineralization of the callorhinchus vertebral column (holocephali; chondrichthyes). *Front. Genet.* 11, 571694. doi: 10.3389/fgene.2020.571694

Prieto, G. (2023). Shark fisheries during the second millennium BC in Gramalote, north coast of Peru. *J. Isl. Coast. Archaeol.* 18, 165–195. doi: 10.1080/15564894.2021.1910386

Rama, S., and Chandrakasan, G. (1984). Distribution of different molecular Species of collagen in the vertebral cartilage of shark (carcharius acutus). *Connect. Tissue Res.* 12, 111–118. doi: 10.3109/03008208408992776

Ricard-Blum, S. (2011). The collagen family. *Cold Spring Harb. Perspect. Biol.* 3 (1), a004978–a004978. doi: 10.1101/cshperspect.a004978

Richter, K. K., Wilson, J., Jones, A. K. G., Buckley, M., Van Doorn, N., and Collins, M. J. (2011). Fish 'n chips: ZooMS peptide mass fingerprinting in a 96 well plate format to identify fish bone fragments. *J. Archaeol. Sci.* 38, 1502–1510. doi: 10.1016/j.jas.2011.02.014

Rick, T. C., Erlandson, J. M., Glassow, M. A., and Moss, M. L. (2002). Evaluating the economic significance of sharks, skates, and rays (elasmobranchs) in prehistoric economies. *J. Archaeol. Sci.* 29, 111–122. doi: 10.1006/jasc.2000.0637

Roff, G., Brown, C. J., Priest, M. A., and Mumby, P. J. (2018). Decline of coastal apex shark populations over the past half century. *Commun. Biol.* 1, 223. doi: 10.1038/s42003-018-0233-1

Royle, T. C. A., Kennedy, J. R., Guiry, E. J., Jackman, L. S., Shichiza, Y., and Yang, D. Y. (2024). Sharkaeology: expanding understandings of historical Chinese diaspora shark fisheries in Monterey bay, California, through the genetic species identification of archaeological chondrichthyes remains. *Hum. Ecol.* 52, 479–495. doi: 10.1007/s10745-024-00521-5

Seersholm, F. V., Cole, T. L., Grealy, A., Rawlence, N. J., Greig, K., Knapp, M., et al. (2018). Subsistence practices, past biodiversity, and anthropogenic impacts revealed by New Zealand-wide ancient DNA survey. *Proc. Natl. Acad. Sci. U.S.A.* 115, 7771–7776. doi: 10.1073/pnas.1803573115

Seidel, R., Lyons, K., Blumer, M., Zaslansky, P., Fratzl, P., Weaver, J. C., et al. (2016). Ultrastructural and developmental features of the tessellated endoskeleton of elasmobranchs (sharks and rays). *J. Anat.* 229, 681–702. doi: 10.1111/joa.12508

Serena, F., Abella, A. J., Bargnesi, F., Barone, M., Colloca, F., Ferretti, F., et al. (2020). Species diversity, taxonomy and distribution of chondrichthyes in the Mediterranean and Black Sea. *The Euro. Zoolog. J.* 87, 497–536. doi: 10.1080/24750263.2020.1805518

Shepherd, L. D., and Campbell, M. (2021). Ancient DNA analysis of an archaeological assemblage of chondrichthyes vertebrae from south Auckland, New Zealand. *J. Archaeol. Sci. Rep.* 36, 102830. doi: 10.1016/j.jasrep.2021.102830

Sherman, C. S., Simpfendorfer, C. A., Pacoureau, N., Matsushiba, J. H., Yan, H. F., Walls, R. H. L., et al. (2023). Half a century of rising extinction risk of coral reef sharks and rays. *Nat. Commun.* 14, 15. doi: 10.1038/s41467-022-35091-x

Smith, S. (2005). Leopard shark mating observed off La Jolla, California. *Calif. Fish Game* 91, 128–135.

Strong, W. R. (1989). *Behavioral Ecology of Horn Sharks, Heterodontus Francisci, at Santa Catalina Island, California, with Emphasis on Patterns of Space Utilization*. Long Beach: California State University.

Weigmann, S., Didier, D., Finucci, B., Nakaya, K., Naylor, G. J. P., Séret, B., et al. (2024). "Biodiversity, taxonomy, and systematics of extant chondrichthyan fishes," in *The Global status of Sharks, Rays, and Chimaeras*, eds. R.W. Jabado, A.Z.A. Morata, R.H. Bennett, B. Finucci, J.R. Ellis, S.L. Fowler, M.I. Grant, A.P. Barbosa Martins S.L. Sinclair and IUCN/SSC Shark Specialist Group (Gland, Switzerland and Cambridge, UK: IUCN), 7–30.

Winn, J. C., Maduna, S. N., and Bester-van der Merwe, A. E. (2024). A comprehensive phylogenomic study unveils evolutionary patterns and challenges in the mitochondrial genomes of carcharhiniformes: a focus on Triakidae. *Genomics* 116, 110771. doi: 10.1016/j.ygeno.2023.110771

Winter, R. M., De Kock, W., Mackie, M., Ramsøe, M., Desiderà, E., Collins, M., et al. (2023). Grouping groupers in the Mediterranean: ecological baselines revealed by ancient proteins. *Ecol. Evol.* 13, e10625. doi: 10.1002/ece3.10625

Worm, B., Orofino, S., Burns, E. S., D'Costa, N. G., Manir Feitosa, L., Palomares, M. L. D., et al. (2024). Global shark fishing mortality still rising despite widespread regulatory change. *Science* 383, 225–230. doi: 10.1126/science.adf8984